*fractal and fractional*

MDPI

*Article*

# The Effects of Thermal Memory on a Transient MHD Buoyancy-Driven Flow in a Rectangular Channel with Permeable Walls: A Free Convection Flow with a Fractional Thermal Flux

**Nehad Ali Shah [1], Bander Almutairi [2], Dumitru Vieru [3,*] and Ahmed A. El-Deeb [4]**

[1] Department of Mechanical Engineering, Sejong University, Seoul 05006, Republic of Korea; nehadali199@sejong.ac.kr
[2] Department of Mathematics, College of Sciences, King Saud University, P.O. Box 2455, Riyadh 11451, Saudi Arabia; baalmutairi@ksu.edu.sa
[3] Department of Theoretical Mechanics, Technical University of Iasi, 700050 Iași, Romania
[4] Department of Mathematics, Faculty of Science, Al-Azhar University, Nasr City, Cairo 11884, Egypt; ahmedeldeeb@zhar.edu.eg
* Correspondence: dumitru.vieru@tuiasi.ro

**Abstract:** This study investigates the effects of magnetic induction, ion slip and Hall current on the flow of linear viscous fluids in a rectangular buoyant channel. In a hydro-magnetic flow scenario with permeable and conducting walls, one wall has a temperature variation that changes over time, while the other wall keeps a constant temperature; the research focuses on this situation. Asymmetric wall heating and suction/injection effects are also examined in the study. Using the Laplace transform, analytical solutions in the Laplace domain for temperature, velocity and induced magnetic field have been determined. The Stehfest approach has been used to find numerical solutions in the real domain by reversing Laplace transforms. The generalized thermal process makes use of an original fractional constitutive equation, in which the thermal flux is influenced by the history of temperature gradients, which has an impact on both the thermal process and the fluid's hydro-magnetic behavior. The influence of thermal memory on heat transfer, fluid movement and magnetic induction was highlighted by comparing the solutions of the fractional model with the classic one based on Fourier's law.

**Keywords:** fractional thermal flux; Caputo derivative; suction/injection; conducting walls; Hall current; Laplace transform



**Citation:** Shah, N.A.; Almutairi, B.; Vieru, D.; El-Deeb, A.A. The Effects of Thermal Memory on a Transient MHD Buoyancy-Driven Flow in a Rectangular Channel with Permeable Walls: A Free Convection Flow with a Fractional Thermal Flux. *Fractal Fract.* **2023**, *7*, 664. https://doi.org/10.3390/fractalfract7090664

Academic Editors: Jordan Hristov, Lanre Akinyemi and Mehmet Senol

Received: 12 July 2023
Revised: 8 August 2023
Accepted: 31 August 2023
Published: 1 September 2023



## 1. Introduction

In nature and industrial processes, magnetic fields influence the behavior of electrically conducting fluids. The magnetic field can induce currents into a moving, electrically conducting fluid, and this creates forces acting on the fluid altering the magnetic field itself. Magneto-hydrodynamics (MHD) describes the macroscopic behavior of a conducting fluid by coupling Maxwell's equations of electromagnetism with hydrodynamics. In magneto-hydrodynamics, the flow of an electrically conducting fluid is governed by the Navier–Stokes equations of fluid dynamics and Maxwell's equations of classical electromagnetism. A consistent set of MHD equations connects the fluid mass density $\rho$, the fluid velocity $\vec{V}$, the thermodynamic pressure $p$ and the magnetic field $\vec{H}$. In derivations of MHD, one should neglect the motion of electrons and consider only heavy ions [1]. This is due to its importance in several scientific and commercial domains, the magnetohydrodynamic flow of an electrically conducting fluid has generated a lot of attention in both theoretical and applied studies. Additionally, it has several uses in MHD power generation, geothermal source research, the cleanup of nuclear fuel waste, plasma research, and high-speed aircraft investigations. Magnetohydrodynamics has a variety of uses in biological and medical

systems. Using magnetic forces to direct therapeutic drugs to particular parts of the body is one example of magnetic therapeutic targeting. MHD can be used to modify blood flow during surgical operations, assuring the patient's health. MHD is also employed to efficiently transport complicated bio-waste fluids. Additionally, magnetic fields are used as a non-invasive therapy approach to manage digestive issues. Chemical and metallurgical engineering processes frequently use MHD effects. Researchers considering various hydromagnetic flows should consult [2–5]. The Hall current is an electrical current that develops when a magnetic field is applied at a right angle to an electric field. Charged particles move along distinct paths that are perpendicular to both fields as a result of the electromagnetic force produced. The impact of the Hall current is often ignored when applied weak to moderate magnetic fields [6,7].

Fractional calculus theory is needed to fill the gap left by the absence of precise models for memory-related events, which are frequently disregarded. Significant recent progress in the modeling of memory effects has been made. Mathematical models based on fractional differential equations have proven their usefulness in describing many complex processes in fluid dynamics, heat and mass transfer. The fractional constitutive equations are able to highlight the influence of the history of the velocity gradients on the fluid movement and the influence of the history of the temperature gradient on the heat transfer process. The choice of different kernels in the definition of fractional operators is essential for the description of complex processes in fluid dynamics with complex structure. Fractional models with the fractional constitutive equation of mass flow are effective in optimizing the study of nanofluids.

Singular operators and nonsingular operators are two types of operators in fractional calculus. Singular operators include the Caputo derivative and the Riemann–Liouville derivative. Non-singular operators include the Caputo–Fabrizio derivative and the Atangana–Baleanu derivative. They developed as a result of the notion of non-local derivatives being applied to traditional differentiation. According to some topic experts, results produced using fractional operators are more accurate and realistic than those obtained using traditional differentiation. Due to their self-similar characteristics and memory-capture abilities, fractional operators are crucial for understanding fluid performance. In the literature on fractional calculus, the Caputo derivative is the one that is most frequently used. This derivative's consistency with the beginning circumstances used to represent real-world problems is the basis for the justification [8,9].

Even though there have been several studies on the natural convection flow of an electrically conducting fluid in channels, the flow in microchannels has received far less attention. For instance, Jha et al. [10] looked into how the flow of a conducting fluid in a vertical parallel plate microchannel was impacted by a transverse magnetic field. They discovered that lowering the Hartmann number resulted in a decrease in the volume flow rate. Jha et al. [11] looked at how a transverse magnetic field that was externally provided and suction/injection may affect a conducting fluid's steady natural convection flow. They found that these effects intensified as the wall–ambient temperature difference ratio decreased. Engineering applications for the free convection flow between two vertical parallel walls include solar energy collection, heat exchanger design, nuclear reactor cooling, electronic equipment cooling, geothermal systems, and many more. Due to the importance of these flows for industry, specialists in fluid mechanics and heat transfer have studied and all have found interesting findings [12,13].

In recent years some excellent works on the using fractional calculus in transport processes have been published.

Hristov [14] investigated the fractional mixed time–space Riemann–Liouville derivatives-based transient flow of a second-grade fluid. An enhanced integral-balance technique has been successful in solving the generalized first Stokes issue. Hristov [15] has investigated diffusion models with fading memory defined by weakly singular kernels using the integral-balance approach. Baleanu et al. [16] have described mathematical models that employ fractional calculus together with numerical approaches to fractional differential

equations. Fractional calculus applications in quantum dynamics, statistical physics and condensed matter physics were given by Tarasov [17]. Atanackovic et al. [18] investigated issues with non-local elasticity, viscoelasticity, heat conduction (diffusion) and many other fascinating problems.

In this work, how the heat memory affects the behavior of buoyancy-driven flow in a rectangular channel with permeable and conducting walls is examined. The study takes a variety of factors into account, such as magnetic induction, ion slip and Hall current. We study the flow of a linear viscous fluid under hydro-magnetic conditions, taking into consideration the asymmetrical heating of the walls and incorporating suction or injection. In our scenario, one of the channel walls' temperatures varies over time, while the other side keeps its temperature constant. This method enables us to address a broad variety of theoretical and practical issues. We build analytical solutions in the Laplace domain for temperature, velocity and induced magnetic fields using the Laplace transform. We use the Stehfest method to invert the Laplace transforms and obtain numerical solutions in the real domain. In our study, a generalized thermal process is paired with a new fractional constitutive equation that explains the thermal flow. This equation takes into account the historical effects of temperature gradients on the fluid's thermal process and hydro-magnetic behavior. By comparing the solutions of the fractional model with those of the traditional model based on Fourier's law, we demonstrate the significant impact of thermal memory on heat transfer, fluid motion, and magnetic induction. The present work has a remarkable degree of novelty. First of all, the consideration of the generalized thermal process allows comparing the results from the classic case, based on Fourier's law, with the results corresponding to the thermal diffusion process described by the generalized thermal flow. On the other hand, the investigation of the influence of the generalized thermal process on the induced magnetic field and on the movement of the fluid is a novelty in specialized literature.

This paper is organized as follows: The formulations of the problem in the dimensional and nondimensional cases along with the fractional model of the thermal process are given in Section 2. Then, in Section 3, we determine analytical solutions in the Laplace domain for the temperature, velocity and magnetic fields. In Section 4, we present numerical results in the real domain for fluid temperature, fluid velocity and induced magnetic field. Section 5 contains the main conclusions of this paper and possible directions for future research involving the new model.

## 2. Statement of the Problem

The transient hydromagnetic flows and heat transfer under effects of Hall and ion slip current in a vertical rectangular channel with conducting/non-conducting porous walls are investigated; see Figure 1. The temperature of the wall $\widetilde{y} = d$ is $\widetilde{T}_d = T_0 + (T_1 - T_0)\widetilde{f}(\widetilde{t})$, $T_1 > T_0$, $\widetilde{f}(0) = 0, \widetilde{f}(\widetilde{t}) > 0, \widetilde{t} > 0$, while the temperature of wall $\widetilde{y} = 0$ is kept at the constant value $T_0$. The velocity field is assumed depending on $\widetilde{y}$ and $\widetilde{t}$, i.e., $\vec{V} = \widetilde{u}(\widetilde{y},\widetilde{t})\,\vec{e}_{\widetilde{x}} + \widetilde{v}(\widetilde{y},\widetilde{t})\,\vec{e}_{\widetilde{y}} + \widetilde{w}(\widetilde{y},\widetilde{t})\,\vec{e}_{\widetilde{z}}$.

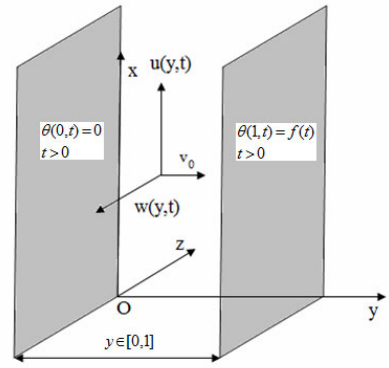


**Figure 1.** Schematic representation of the flow domain (dimensionless coordinates).

The continuity equation $\frac{\partial \widetilde{u}}{\partial \widetilde{x}} + \frac{\partial \widetilde{v}}{\partial \widetilde{y}} + \frac{\partial \widetilde{w}}{\partial \widetilde{z}} = 0$ implies that the velocity component $\widetilde{v}$ has to satisfy condition $\frac{\partial \widetilde{v}}{\partial \widetilde{y}} = 0$. In the present paper, a constant section/injection velocity is considered; therefore, the velocity vector field is given by $\overrightarrow{V} = \left(\widetilde{u}(\widetilde{y},\widetilde{t}), -\widetilde{v}_0,\ \widetilde{w}(\widetilde{y},\widetilde{t})\right)$. The magnetic field is assumed of the type $\overrightarrow{H} = \left(\widetilde{H}_{\widetilde{x}}(\widetilde{y},\widetilde{t}),\ \widetilde{H}_0,\ \widetilde{H}_{\widetilde{z}}(\widetilde{y},\widetilde{t})\right)$, and it is considered to be significant enough to impact Hall and ion slip current in a direction opposite the induced electric and magnetic fields. In the above assumptions and the Boussinesq approximation, the governing flow equation are [1–3]

$$\rho\left(\frac{\partial \widetilde{u}}{\partial \widetilde{t}} - \widetilde{v}_0\frac{\partial \widetilde{u}}{\partial \widetilde{y}}\right) = \mu\frac{\partial^2 \widetilde{u}}{\partial \widetilde{y}^2} + \mu_e \widetilde{H}_0\frac{\partial \widetilde{H}_{\widetilde{x}}}{\partial \widetilde{y}} + \rho g\beta(\widetilde{T} - T_0), \tag{1}$$

$$\rho\left(\frac{\partial \widetilde{w}}{\partial \widetilde{t}} - \widetilde{v}_0\frac{\partial \widetilde{w}}{\partial \widetilde{y}}\right) = \mu\frac{\partial^2 \widetilde{w}}{\partial \widetilde{y}^2} + \mu_e \widetilde{H}_0\frac{\partial \widetilde{H}_{\widetilde{z}}}{\partial \widetilde{y}}, \tag{2}$$

$$\frac{\partial \widetilde{H}_{\widetilde{x}}}{\partial \widetilde{t}} = \nu_m(1+\beta_e\beta_i)\frac{\partial^2 \widetilde{H}_{\widetilde{x}}}{\partial \widetilde{y}^2} + \widetilde{H}_0\frac{\partial \widetilde{u}}{\partial \widetilde{y}} - \beta_e\nu_m\frac{\partial^2 \widetilde{H}_{\widetilde{z}}}{\partial \widetilde{y}^2} + \widetilde{v}_0\frac{\partial \widetilde{H}_{\widetilde{x}}}{\partial \widetilde{y}}, \tag{3}$$

$$\frac{\partial \widetilde{H}_{\widetilde{z}}}{\partial \widetilde{t}} = \nu_m(1+\beta_e\beta_i)\frac{\partial^2 \widetilde{H}_{\widetilde{z}}}{\partial \widetilde{y}^2} + \widetilde{H}_0\frac{\partial \widetilde{w}}{\partial \widetilde{y}} + \beta_e\nu_m\frac{\partial^2 \widetilde{H}_{\widetilde{x}}}{\partial \widetilde{y}^2} + \widetilde{v}_0\frac{\partial \widetilde{H}_{\widetilde{z}}}{\partial \widetilde{y}}, \tag{4}$$

$$\rho c_p\left(\frac{\partial \widetilde{T}}{\partial \widetilde{t}} - \widetilde{v}_0\frac{\partial \widetilde{T}}{\partial \widetilde{y}}\right) = -\frac{\partial \widetilde{q}}{\partial \widetilde{y}}, \tag{5}$$

$$\widetilde{q} = -k\frac{\partial \widetilde{T}}{\partial \widetilde{y}}, \tag{6}$$

where the significance of the used parameters is given in the nomenclature.

Along with Equations (1)–(6), we consider the initial and boundary conditions:

$$\widetilde{u}(\widetilde{y},0) = \widetilde{w}(\widetilde{y},0) = 0,\ \widetilde{H}_{\widetilde{x}}(\widetilde{y},0) = \widetilde{H}_{\widetilde{z}}(\widetilde{y},0) = 0,\ \widetilde{T}(\widetilde{y},0) = T_0, \tag{7}$$

$$\widetilde{u}(0,\widetilde{t}) = \xi\left.\frac{\partial \widetilde{u}(\widetilde{y},\widetilde{t})}{\partial \widetilde{y}}\right|_{\widetilde{y}=0},\ \widetilde{w}(0,\widetilde{t}) = \xi\left.\frac{\partial \widetilde{w}(\widetilde{y},\widetilde{t})}{\partial \widetilde{y}}\right|_{\widetilde{y}=0},\ \widetilde{t} > 0, \tag{8}$$

$$b_1\left.\frac{\partial \widetilde{H}_{\widetilde{x}}(\widetilde{y},\widetilde{t})}{\partial \widetilde{y}}\right|_{\widetilde{y}=0} + b_2\widetilde{H}_{\widetilde{x}}(0,\widetilde{t}) = 0,\ \mathrm{b}_1\left.\frac{\partial \widetilde{H}_{\widetilde{z}}(\widetilde{y},\widetilde{t})}{\partial \widetilde{y}}\right|_{\widetilde{y}=0} + b_2\widetilde{H}_{\widetilde{z}}(0,\widetilde{t}) = 0, \widetilde{t} > 0, \tag{9}$$

$$\widetilde{T}(0,\widetilde{t}) = T_0,\ \widetilde{t} > 0, \tag{10}$$

$$\widetilde{u}(d,\widetilde{t}) = -\xi\left.\frac{\partial \widetilde{u}(\widetilde{y},\widetilde{t})}{\partial \widetilde{y}}\right|_{\widetilde{y}=d},\ \widetilde{w}(d,\widetilde{t}) = -\xi\left.\frac{\partial \widetilde{w}(\widetilde{y},\widetilde{t})}{\partial \widetilde{y}}\right|_{\widetilde{y}=d},\ \widetilde{t} > 0, \tag{11}$$

$$b_3\left.\frac{\partial \widetilde{H}_{\widetilde{x}}(\widetilde{y},\widetilde{t})}{\partial \widetilde{y}}\right|_{\widetilde{y}=d} + b_4\widetilde{H}_{\widetilde{x}}(d,\widetilde{t}) = 0,\ \mathrm{b}_3\left.\frac{\partial \widetilde{H}_{\widetilde{z}}(\widetilde{y},\widetilde{t})}{\partial \widetilde{y}}\right|_{\widetilde{y}=d} + b_4\widetilde{H}_{\widetilde{z}}(d,\widetilde{t}) = 0, \widetilde{t} > 0, \tag{12}$$

$$\widetilde{T}(d,\widetilde{t}) = T_0 + (T_1 - T_0)\widetilde{f}(\widetilde{t}),\ \widetilde{t} > 0. \tag{13}$$

where $b_i,\ i = 1, 2, \ldots, 4$ and $\xi$ are known constants.

From the use of nondimensional parameters and functions,

$$\left.\begin{array}{l}(x,y,z)=\frac{1}{d}(\widetilde{x},\widetilde{y},\widetilde{z}),\ t=\frac{\nu}{d^2}\widetilde{t},\ (u,w)=\frac{\nu}{gd^2\beta(T_1-T_0)}(\widetilde{u},\widetilde{v}),\ v_0=\frac{d\widetilde{v}_0}{\nu},\\ (H_x,H_z)=\frac{\nu}{gd^2\beta(T_1-T_0)}\sqrt{\frac{\mu_e}{\rho}}(\widetilde{H}_{\widetilde{x}},\widetilde{H}_{\widetilde{z}}),\ M_0=\frac{d\widetilde{H}_0}{\nu}\sqrt{\frac{\mu_e}{\rho}},\ p_m=\frac{\nu_m}{\nu}(1+\beta_e\beta_i),\\ q_m=\frac{\nu_m}{\nu}\beta_e,\ \nu_m=\sigma\mu_e,\ q=\frac{d}{k(T_1-T_0)}\widetilde{q},\ \theta=\frac{\widetilde{T}-T_0}{T_1-T_0},\ \mathrm{Pr}=\frac{\mu c_p}{k},\ \xi_0=\frac{\xi}{d},\\ \beta_1=\frac{b_1}{d},\ \beta_2=b_2,\ \beta_3=\frac{b_3}{d},\ \beta_4=b_4,\ f(t)=\widetilde{f}\left(\frac{d^2}{\nu}t\right),\end{array}\right\} \tag{14}$$

we obtain

$$\frac{\partial u}{\partial t}=\frac{\partial^2 u}{\partial y^2}+v_0\frac{\partial u}{\partial y}+M_0\frac{\partial H_x}{\partial y}+\theta, \tag{15}$$

$$\frac{\partial w}{\partial t}=\frac{\partial^2 w}{\partial y^2}+v_0\frac{\partial w}{\partial y}+M_0\frac{\partial H_z}{\partial y}, \tag{16}$$

$$\frac{\partial H_x}{\partial t}=p_m\frac{\partial^2 H_x}{\partial y^2}-q_m\frac{\partial^2 H_z}{\partial y^2}+M_0\frac{\partial u}{\partial y}+v_0\frac{\partial H_x}{\partial y}, \tag{17}$$

$$\frac{\partial H_z}{\partial t}=p_m\frac{\partial^2 H_z}{\partial y^2}+q_m\frac{\partial^2 H_x}{\partial y^2}+M_0\frac{\partial w}{\partial y}+v_0\frac{\partial H_z}{\partial y}, \tag{18}$$

$$\mathrm{Pr}\frac{\partial \theta}{\partial t}-\mathrm{Pr}v_0\frac{\partial \theta}{\partial y}=-\frac{\partial q}{\partial y}, \tag{19}$$

$$q=-\frac{\partial \theta}{\partial y}. \tag{20}$$

The dimensionless initial and boundary conditions are

$$u(y,0)=w(y,0)=0,\ H_x(y,0)=H_z(y,0)=0,\ \theta(y,0)=0, \tag{21}$$

$$u(0,t)=\xi_0\left.\frac{\partial u(y,t)}{\partial y}\right|_{y=0},\ w(0,t)=\xi_0\left.\frac{\partial w(y,t)}{\partial y}\right|_{y=0},\ t>0, \tag{22}$$

$$\beta_1\left.\frac{\partial H_x(y,t)}{\partial y}\right|_{y=0}+\beta_2 H_x(0,t)=0,\ \beta_1\left.\frac{\partial H_z(y,t)}{\partial y}\right|_{y=0}+\beta_2 H_z(0,t)=0, t>0, \tag{23}$$

$$\theta(0,t)=0,\ t>0, \tag{24}$$

$$u(1,t)=-\xi_0\left.\frac{\partial u(y,t)}{\partial y}\right|_{y=1},\ w(1,t)=-\xi_0\left.\frac{\partial w(y,t)}{\partial y}\right|_{y=1},\ t>0, \tag{25}$$

$$\beta_3\left.\frac{\partial H_x(y,t)}{\partial y}\right|_{y=1}+\beta_4 H_x(1,t)=0,\ \beta_3\left.\frac{\partial H_z(y,t)}{\partial y}\right|_{y=1}+\beta_4 H_z(1,t)=0, t>0, \tag{26}$$

$$\theta(1,t)=f(t). \tag{27}$$

*Fractional Constitutive Equation of the Thermal Flux*

In this section, we propose a fractional constitutive equation instead of the classical Fourier law given by Equation (6), respectively (20). First, we present some basic elements about the time-fractional Caputo derivative necessary to approach our problem.

**Definition 1.** *The Riemann-Liouville kernel is defined as [19]*

$${}_{RL}k(t,\alpha)=\begin{cases}\frac{t^{\alpha-1}}{\Gamma(\alpha)},\ t>0,\ \alpha>0,\\ \delta(t),\ t>0,\ \alpha=0,\end{cases} \tag{28}$$

*where* $\Gamma(\cdot)$ *is Gamma function, and* $\delta(\cdot)$ *is Dirac's distribution.*

Denoting by $\overline{\psi}(s,\alpha) = \int_0^\infty \psi(t,\alpha)e^{-st}ds = L\{\psi(t,\alpha)\}$, the Laplace transform is $\psi(t,\alpha)$, and it is obtained that the Laplace transform of the Riemann–Liouville kernel is

$$_{RL}\overline{k}(s,\alpha) = s^{-\alpha},\ \alpha \geq 0. \tag{29}$$

Let $\upsilon(y,t)$ be a differentiable function $\upsilon : [0,\infty) \times [0,\infty) \to \mathbb{R}$.

**Definition 2.** *The Riemann–Liouville fractional integral of function* $\upsilon(y,t)$ *is defined as*

$$I_t^\alpha \upsilon(y,t) = {}_{RL}k(t,\alpha) * \upsilon(y,t) = \int_0^t \frac{(t-\tau)^{\alpha-1}}{\Gamma(\alpha)}\upsilon(y,\tau)d\tau. \tag{30}$$

It is easy to see that:

$$_{RL}I_t^0\upsilon(y,t) = \upsilon(y,t), L\{_{RL}I_t^\alpha\upsilon(y,t)\} = {}_{RL}\overline{k}(s,\alpha)\overline{\upsilon}(y,s) = s^{-\alpha}\overline{\upsilon}(y,s). \tag{31}$$

**Definition 3.** *The Caputo kernel is defined as*

$$_Ck(t,\alpha) = \begin{cases} \frac{t^{-\alpha}}{\Gamma(1-\alpha)},\ t > 0,\ 0 < \alpha < 1, \\ \delta(t),\ t > 0,\ \alpha = 1, \end{cases} \tag{32}$$

The Laplace transform of function ${}_Ck(t,\alpha)$ is

$$_C\overline{k}(t,\alpha) = s^{\alpha-1}. \tag{33}$$

**Definition 4.** *The time-fractional Caputo derivative of function* $\upsilon(y,t)$ *is defined by*

$$_CD_t^\alpha\upsilon(y,t) = {}_Ck(t,\alpha) * \frac{\partial\upsilon(y,t)}{\partial t} = {}_{RL}k(t,1-\alpha) * \frac{\partial\upsilon(y,t)}{\partial t},\ 0 \leq \alpha \leq 1. \tag{34}$$

The properties of the time-fractional Caputo derivative are:

$$_CD_t^1\upsilon(y,t) = \delta(t) * \frac{\partial\upsilon(y,t)}{\partial t} = \frac{\partial\upsilon(y,t)}{\partial t}, \tag{35}$$

$$L\{_CD_t^\alpha\upsilon(y,t)\} = s^{\alpha-1}[s\overline{\upsilon}(y,s) - \upsilon(y,0)], \tag{36}$$

$$_{RL}I_t^\alpha\{_CD_t^\alpha\upsilon(y,t)\} = {}_{RL}k(t,\alpha) * {}_{RL}k(t,1-\alpha) * \frac{\partial\upsilon(y,t)}{\partial t} = \int_0^t \frac{\partial\upsilon(y,\tau)}{\partial\tau}d\tau = \upsilon(y,t) - \upsilon(y,0). \tag{37}$$

The generalized thermal process with the dimensionless thermal flux given by

$$q(y,t) = -_{RL}I_t^\alpha\left(\frac{\partial\theta(y,t)}{\partial y}\right),\ 0 \leq \alpha \leq 1. \tag{38}$$

For $\alpha = 0$ the fractional Equation (38) becomes the classical Equation (20).

## 3. Solution to the Problem

### *3.1. Determination of the Temperature Field*

The temperature field of the generalized problem is given by the solution of the differential Equations (19) and (38), along with the initial Condition (21) and boundary Conditions (24) and (27).

Replacing (38) in Equation (19), we obtain that the nondimensional temperature field $\theta(y,t)$ has to satisfy the fractional differential equation

$$\mathrm{Pr}\frac{\partial\theta}{\partial t} - \mathrm{Pr}v_0\frac{\partial\theta}{\partial y} = {}_{RL}I_t^{\alpha}\left(\frac{\partial^2\theta}{\partial y^2}\right),\ 0 \le \alpha \le 1. \tag{39}$$

We obtain the transformed equation by applying the Laplace transform to the equation given in (39) and take the initial condition showed in (21) into account.

$$\frac{\partial^2\overline{\theta}(y,s)}{\partial y^2} + \mathrm{Pr}v_0 s^{\alpha}\frac{\partial\overline{\theta}(y,s)}{\partial y} - \mathrm{Pr}s^{\alpha+1}\overline{\theta}(y,s) = 0. \tag{40}$$

Making the transformation

$$\overline{\theta}(y,s) = \exp\left(-\frac{\mathrm{Pr}v_0 s^{\alpha}}{2}y\right)\overline{\varphi}(y,s), \tag{41}$$

it results that $\overline{\varphi}(y,s)$ is the solution of the DE.

$$\frac{\partial^2\overline{\varphi}(y,s)}{\partial y^2} = \chi^2(s)\overline{\varphi}(s), \tag{42}$$

where,

$$\chi(s) = \frac{1}{2}\sqrt{\left(\mathrm{Pr}v_0 s^{\alpha} + \frac{2s}{v_0}\right)^2 - \frac{4s^2}{v_0^2}} = \frac{1}{2}\sqrt{\mathrm{Pr}^2 v_0^2 s^{2\alpha} + 4\mathrm{Pr}s^{\alpha+1}}. \tag{43}$$

Function $\overline{\varphi}(y,s)$ has to satisfy the boundary conditions.

$$\overline{\varphi}(0,s) = 0,\ \overline{\varphi}(1,s) = \overline{f}(s)\exp\left(\frac{\mathrm{Pr}v_0 s^{\alpha}}{2}\right), \tag{44}$$

where $\overline{f}(s) = L\{f(t)\}(s)$.

The solution of Equation (42) using (45) is

$$\overline{\varphi}(y,s) = \frac{\sinh(y\chi(s))}{\sinh(\chi(s))}\overline{f}(s)\exp\left(\frac{\mathrm{Pr}v_0 s^{\alpha}}{2}\right). \tag{45}$$

Finally, the Laplace transform of the temperature field is

$$\overline{\theta}(y,s) = \frac{\sinh(y\chi(s))}{\sinh(\chi(s))}\overline{f}(s)\exp\left(\frac{\mathrm{Pr}v_0 s^{\alpha}(1-y)}{2}\right). \tag{46}$$

Expression (46) is complicated; therefore, it is difficult to determine the inverse Laplace transform with classical methods from the complex analysis. To determine the numerical values in the real domain of (46), we will use the Stehfest algorithm.

The particular case $\alpha = 0$ (the classical Fourier's law of thermal flux)

In this case, we obtain $\chi(s) = \frac{1}{2}\sqrt{\mathrm{Pr}^2 v_0^2 + 4\mathrm{Pr}s} = \sqrt{\mathrm{Pr}}\sqrt{s + \frac{\mathrm{Pr}v_0^2}{4}}$. The temperature field (46) can be written as

$$\begin{aligned}\overline{\theta}(y,s) &= \mathrm{e}^{(\frac{\mathrm{Pr}v_0(1-y)}{2})}\overline{f}(s)\frac{\sinh(y\sqrt{\mathrm{Pr}}\sqrt{s+C_0})}{\sinh(\sqrt{\mathrm{Pr}}\sqrt{s+C_0})} = \mathrm{e}^{(\frac{(1-y)\mathrm{Pr}v_0}{2})}\overline{f}(s)\sum_{k=0}^{\infty}\left[e^{-(2k+1-y)\sqrt{\mathrm{Pr}}\sqrt{s+C_0})} - e^{-(2k+1+y)\sqrt{\mathrm{Pr}}C_0)}\right] \\ &= \mathrm{e}^{(\frac{(1-y)\mathrm{Pr}v_0}{2})}(s+C_0)\overline{f}(s)\sum_{k=0}^{\infty}\left[\frac{e^{-\sqrt{\mathrm{Pr}}(2k+1-y)\sqrt{s+C_0})}}{s+C_0} - \frac{e^{-\sqrt{\mathrm{Pr}}(2k+1+y)\sqrt{s+C_0})}}{s+C_0}\right].\end{aligned} \tag{47}$$

Using formulas

$$L^{-1}\left\{\frac{e^{-a\sqrt{s+C_0}}}{s+C_0}\right\} = e^{-C_0t}erfc\left(\frac{a}{2\sqrt{t}}\right), \text{if } f(0)=0 \Rightarrow L^{-1}\left\{s\overline{f}(s)\right\} = f'(t),$$

we obtain the temperature field

$$\theta(y,t) = \mathrm{e}^{(\frac{(1-y)\mathrm{Pr}v_0}{2})}[f'(t)+C_0f(t)] * \sum_{k=0}^{\infty}e^{-C_0t}\left[erfc\left(\frac{(2k+1-y)\sqrt{\mathrm{Pr}}}{2\sqrt{t}}\right) - erfc\left(\frac{(2k+1+y)\sqrt{\mathrm{Pr}}}{2\sqrt{t}}\right)\right], \tag{48}$$

where $C_0 = \frac{\mathrm{Pr}v_0^2}{4}$, and $erfc(z) = \frac{2}{\sqrt{\pi}}\int_z^{\infty}\exp(-u^2)du$ is the complementary Gauss error function.

*3.2. Determination of the Velocity and Induced Magnetic Fields*

Introducing the complex fields $v = u + iw$, $H = H_x + iH_z$, Equations (15)–(18) are written as

$$\frac{\partial v}{\partial t} = \frac{\partial^2 v}{\partial y^2} + \mathrm{v}_0\frac{\partial v}{\partial y} + M_0\frac{\partial H}{\partial y} + \theta, \tag{49}$$

$$\frac{\partial H}{\partial t} = p_m\frac{\partial^2 H}{\partial y^2} + iq_m\frac{\partial^2 H}{\partial y^2} + M_0\frac{\partial v}{\partial y} + \mathrm{v}_0\frac{\partial H}{\partial y}. \tag{50}$$

Functions $v(y,t)$, $H(y,t)$ have to satisfy the initial and boundary conditions

$$v(y,0) = 0, H(y,0) = 0, \tag{51}$$

$$v(0,t) = \xi_0\frac{\partial v(y,t)}{\partial y}\big|_{y=0}, t > 0, \tag{52}$$

$$\beta_1\frac{\partial H(y,t)}{\partial y}\big|_{y=0} + \beta_2 H(0,t) = 0, t > 0, \tag{53}$$

$$v(1,t) = -\xi_0\frac{\partial v(y,t)}{\partial y}\big|_{y=1}, t > 0, \tag{54}$$

$$\beta_3\frac{\partial H(y,t)}{\partial y}\big|_{y=1} + \beta_4 H(1,t) = 0, t > 0. \tag{55}$$

Applying the Laplace transform to Equations (49) and (50), and using the initial Conditions (51), we obtain the transformed equations

$$\frac{\partial^2\overline{v}(y,s)}{\partial y^2} + \mathrm{v}_0\frac{\partial\overline{v}(y,s)}{\partial y} - s\overline{v}(y,s) + M_0\frac{\partial\overline{H}(y,s)}{\partial y} + \overline{\theta}(y,s) = 0, \tag{56}$$

$$r_m\frac{\partial^2\overline{H}(y,s)}{\partial y^2} + M_0\frac{\partial\overline{v}(y,s)}{\partial y} - s\overline{H}(y,s) + \mathrm{v}_0\frac{\partial\overline{H}}{\partial y} = 0. \tag{57}$$

Now, we write Equations (56) and (57) in the equivalent forms

$$\frac{\partial\overline{H}}{\partial y} = {M_0}^{-1}\left[s\overline{v} - \theta - \mathrm{v}_0\frac{\partial^2\overline{v}}{\partial y^2}\right], \tag{58}$$

$$M_0\frac{\partial^2\overline{v}}{\partial y^2}+r_m\frac{\partial^2}{\partial y^2}\left(\frac{\partial\overline{H}}{\partial y}\right)+\mathrm{v}_0\frac{\partial}{\partial y}\left(\frac{\partial\overline{H}}{\partial y}\right)-s\frac{\partial H}{\partial y}=0. \tag{59}$$

Replacing (58) into (59), we obtain that the function $\overline{v}(y,s)$ has to satisfy the following differential equation:

$$r_m\frac{\partial^4\overline{v}}{\partial y^4}+(1+r_m)\mathrm{v}_0\frac{\partial^3\overline{v}}{\partial y^3}-\left[(1+r_m)s+M_0^2-\mathrm{v}_0^2\right]\frac{\partial^2\overline{v}}{\partial y^2}-2\mathrm{v}_0s\frac{\partial\overline{v}}{\partial y}+s^2\overline{V}=\overline{F}(y,s), \tag{60}$$

where

$$\overline{F}(y,s)=s\overline{\theta}-v_0\frac{\partial\overline{\theta}}{\partial y}-r_m\frac{\partial^2\overline{\theta}}{\partial y^2}=\frac{\overline{f}(s)}{\sinh(w(s))}\exp[\gamma_0(s)(1-y)][\gamma_1(s)\cosh(yw(s))+\gamma_2(s)\sinh(yw(s))], \tag{61}$$

$$\gamma_0(s)=\frac{1}{2}\mathrm{Pr}v_0s^\alpha,\ \gamma_1(s)=(r_m\mathrm{Pr}v_0s^\alpha-v_0)w(s),\ \gamma_2(s)=(v_0-r_m)\gamma_0(s)-r_mw^2(s). \tag{62}$$

A particular solution of Equation (60) is

$$\overline{v}_p(y,s)=\exp[\gamma_0(s)(1-y)][\overline{v}_{p_1}(s)\cosh(yw(s))+\overline{v}_{p_2}(s)\sinh(yw(s))], \tag{63}$$

where functions $\overline{v}_{p_1}(s),\ \overline{v}_{p_1}(s)$ are given by

$$\begin{array}{l}\overline{v}_{p_1}(s)=\frac{\overline{f}(s)[a_{22}(s)\gamma_1(s)-a_{12}(s)\gamma_2(s)]}{\sinh(w(s))[a_{11}(s)a_{22}(s)-a_{12}(s)a_{21}(s)]},\\ \overline{v}_{p_2}(s)=\frac{\overline{f}(s)[a_{11}(s)\gamma_2(s)-a_{21}(s)\lambda_1(s)]}{\sinh(w(s))[a_{11}(s)a_{22}(s)-a_{12}(s)a_{21}(s)]}.\end{array} \tag{64}$$

And $a_{ij}(s),\ i,j=1,2$ are given in Appendix A.

The homogeneous equation associated with the differential Equation (60) has the characteristic equation

$$r_mX^4+(1+r_m)\mathrm{v}_0X^3-[(1+r_m)s+M_0^2-\mathrm{v}_0^2]X^2-2\mathrm{v}_0sX+s^2=0 \tag{65}$$

We denote by $X_i(s), i=1,2,3,4$ the roots of Equation (65), whose expressions are given in Appendix A.

The general solution of Equation (60) is given by

$$\overline{v}(y,s)=\sum_{i=1}^{4}C_i(s)e^{X_i(s)y}+\overline{v}_p(y,s). \tag{66}$$

Using (58), (60) and (66), we obtain the complex magnetic field given by

$$\begin{array}{l}\overline{H}(y,s)=\sum\limits_{i=1}^{4}M_0^{-1}\left(\frac{s}{X_i(s)}-\mathrm{v}_0-X_i(s)\right)C_i(s)e^{X_i(s)y}+\overline{H}_1(s)\exp[\gamma_0(s)(1-y)]\sinh(yw(s))+\\ \quad+\overline{H}_2(s)\exp[\gamma_0(s)(1-y)]\cosh(yw(s)),\end{array} \tag{67}$$

where

$$\begin{array}{l}\overline{H}_1(s)=\frac{M_0^{-1}}{w^2(s)-\gamma_0^2(s)}\Big\{[\overline{v}_{p_1}(s)w(s)+\overline{v}_{p_2}(s)\gamma_0(s)]s-\frac{\overline{f}(s)\gamma_0(s)}{\sinh(w(s))}-[\mathrm{v}_0\overline{v}_{p_2}(s)+\overline{v}_{p_1}(s)w(s)-\\ \quad-\overline{v}_{p_2}(s)\gamma_0(s)](w^2(s)-\gamma_0^2(s))\Big\},\\ \overline{H}_2(s)=\frac{M_0^{-1}}{w^2(s)-\gamma_0^2(s)}\Big\{[\overline{v}_{p_1}(s)\gamma_0(s)+\overline{v}_{p_2}(s)w(s)]s-\frac{\overline{f}(s)w(s)}{\sinh(w(s))}-[\mathrm{v}_0\overline{v}_{p_1}(s)+\overline{v}_{p_2}(s)w(s)-\\ \quad-\overline{v}_{p_1}(s)\gamma_0(s)](w^2(s)-\gamma_0^2(s))\Big\}.\end{array} \tag{68}$$

The integration constants $C_i(s),\ i = 1,2,3,4$ are determined using the boundary Conditions (52)–(55). Applying the Laplace transform to Equations (52)–(55), we obtain the boundary conditions for the functions $\overline{v}(y,s)$ and $\overline{H}(y,s)$, namely

$$\begin{aligned} &\overline{v}(0,s) = \xi_0 \frac{\partial \overline{v}(y,s)}{\partial y}\Big|_{y=0}, \overline{v}(1,s) = -\xi_0 \frac{\partial \overline{v}(y,s)}{\partial y}\Big|_{y=1}, \\ &\beta_1 \frac{\partial \overline{H}(y,s)}{\partial y}\Big|_{y=0} + \beta_2 \overline{H}(0,s) = 0, \beta_3 \frac{\partial \overline{H}(y,s)}{\partial y}\Big|_{y=1} + \beta_4 \overline{H}(1,s) = 0. \end{aligned} \tag{69}$$

Using (63), (66) and (67), the boundary Conditions (69) lead to the following algebraic system for $C_i(s),\ i = 1,2,3,4$ :

$$\boldsymbol{MC} = \boldsymbol{D}, \tag{70}$$

where the matrices $\boldsymbol{M}$, $\boldsymbol{C}$ and $\boldsymbol{D}$ are given in Appendix A. Supposing $\det(\boldsymbol{M}) \neq 0$, the solution of the matriceal Equation (70) is

$$\boldsymbol{C} = \boldsymbol{M}^{-1}\boldsymbol{D}, \tag{71}$$

which is obtained using the symbolic calculus in Mathcad 15.

Obviously, the final expressions of the velocity and magnetic fields are complicated enough. The numerical values of the inverse Laplace transforms will be determined using Stehfest's algorithm [20]. According to this algorithm, the inverse transform $\wp(y,t)$ of the Laplace transform $\overline{\wp}(y,s)$ is given by

$$\wp(y,t) = \frac{\ln 2}{t} \sum_{r=1}^{2p} (-1)^{r+p} \sum_{i=[\frac{r+1}{2}]}^{\min(j,p)} \frac{i^p (2i)!}{i!(p-i)!(i-1)!(r-1)!(2i-r)!} \overline{\wp}\left(y, \frac{r \ln 2}{t}\right), \tag{72}$$

where $p > 0,\ p \in \mathbb{N}$, $\left[\frac{r+1}{2}\right]$ denotes the integer part of the number $\frac{r+1}{2}$ and $\min(r,p) = \frac{r+p-|r-p|}{2}$.

Mathcad 15 software will be used to obtain numerical simulations and graphical representations of functions $\theta(y,t), u(y,t), w(y,t), H_x(y,t)$ and $H_z(y,t)$.

### *3.3. Generalized Nusselt Number and Skin Friction*

In this section, we determine the expressions of two important parameters for practical problems, namely, the Nusselt number and skin friction.

In thermal processes, the Nusselt number is the dimensionless number that characterizes the heat transfer between the solid wall and the fluid. For the model studied in this article, we define the generalized Nusselt numbers on the walls $y = 0,\ y = 1$, as

$$Nu_0(t) = -\frac{\partial}{\partial y}({}_{RL}I_t^{\alpha}\theta(y,t))\Big|_{y=0},\ Nu_1(t) = -\frac{\partial}{\partial y}({}_{RL}I_t^{\alpha}\theta(y,t))\Big|_{y=1}, \tag{73}$$

respectively. Obviously, for $\alpha = 0$, the ordinary Nusselt numbers are obtained.

Applying the Laplace transform to Equation (73) and using Equations (31) and (46), we obtain

$$\overline{N}u_0(s) = -\frac{\exp\left(\frac{\mathrm{Pr}v_0 s^{\alpha}}{2}\right)}{s^{\alpha}\sinh(\chi(s))}\overline{f}(s)\chi(s), \tag{74}$$

$$\overline{N}u_1(s) = -\frac{1}{s^{\alpha}\sinh(\chi(s))}\left[\chi(s)\cosh(\chi(s)) - \frac{\mathrm{Pr}v_0 s^{\alpha}}{2}\sinh(\chi(s))\right]\overline{f}(s). \tag{75}$$

Numerical values of $Nu_0(t)$ and $Nu_1(t)$, in the real domain will be determined using Stehfest's algorithm (72).

The complex skin friction coefficients on the walls are defined as

$$\begin{aligned} C_{f0}(t) &= \left.\frac{\partial v(y,t)}{\partial y}\right|_{y=0} = \left.\frac{\partial u(y,t)}{\partial y}\right|_{y=0} + i\left.\frac{\partial w(y,t)}{\partial y}\right|_{y=0} = C_{fx0} + iC_{fx0}, \\ C_{f1}(t) &= \left.\frac{\partial v(y,t)}{\partial y}\right|_{y=1} = \left.\frac{\partial u(y,t)}{\partial y}\right|_{y=1} + i\left.\frac{\partial w(y,t)}{\partial y}\right|_{y=1} = C_{fx1} + iC_{fx1}. \end{aligned} \tag{76}$$

## 4. Results and Discussion

The objective of this work is to investigate the flow of a Newtonian fluid with convective magnetohydrodynamics (MHD) in a vertical channel using a mathematical model with a fractional constitutive equation for heat flux. The thermal flux in this particular model is affected by the historical evolution of the temperature gradient. The time-fractional derivative of the model employs a power-law dampening kernel. The considered boundary conditions could describe slip/no slip phenomena on the walls. Also, the channel walls could be conducting/non-conducting, are asymmetric heated and micro-porous. The suction/injection velocity is constant equal to $v_0$.

Analytical solutions for temperature, velocity and induced magnetic fields have been obtained in the Laplace domain by considering the time-dependent temperature on the wall $\widetilde{y} = d$.

To highlight the influence of the thermal memory on the thermal transport, numerical simulations have been carried out in the case when the channel walls are kept at the constant non-dimensional temperatures $\theta(0,t) = 0$, respectively $\theta(1,t) = 1$. The numerical values of the temperature are determined using Formula (46) and the Stehfest algorithm for the inversion of the Laplace transforms.

Figure 2 was drawn in order to highlight the evolution over time of the fluid temperature in various positions in the channel. It is important to note that the temperature values vary significantly only for a short period of time, after which stabilization occurs towards a constant value for each position in the channel.

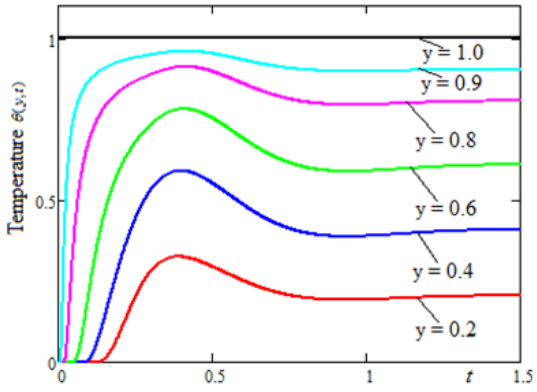


**Figure 2.** Time-variation on $\theta(y,t)$ for $\alpha = 0.5, \mathrm{Pr} = 0.5, v_0 = 0.05$.

This property, highlighted by the curves in Figure 2, is also theoretically justified based on the following property of the Laplace transform: $\lim_{t\to\infty} f(t) = \lim_{s\to 0} sF(s)$, where $F(s)$ is the Laplace transform of function $f(t)$. Applying the above property to the temperature Laplace transform $\overline{\theta}(y,s)$ given by Equation (46), we have that $\lim_{t\to\infty} \theta(y,t) = \lim_{s\to 0} s\overline{\theta}(y,s) = y$; therefore, the permanent solution for temperature (the post-transitory solution) is $\theta_{st}(y) = y$.

The fluid temperature property, discussed above and highlighted by the curves in Figure 2, is also clearly presented in Table 1. In this table, the temperature values for $y \in \{0.2, 0.4, 0.6, 0.8, 0.9, 1.0\}$ and for increasing time values are presented. It was observed that, depending on the desired precision, the transient stage could be considered finished at the time $t = 350$.

**Table 1.** Values of $\theta(y,t)$ for large values $t$.

| | $\theta(y,t)$ | | | | | | |
|---|---|---|---|---|---|---|---|
| | $t = 1.5$ | $t = 3.5$ | $t = 9.5$ | $t = 13.5$ | $t = 15.5$ | $t = 19.5$ | $t = 350$ |
| $y = 0.2$ | 0.20536 | 0.20118 | 0.20052 | 0.20040 | 0.20036 | 0.20031 | 0.20006 |
| $y = 0.4$ | 0.40880 | 0.40193 | 0.40082 | 0.40062 | 0.40056 | 0.40047 | 0.40009 |
| $y = 0.6$ | 0.60934 | 0.60210 | 0.60086 | 0.60064 | 0.60058 | 0.60049 | 0.60009 |
| $y = 0.8$ | 0.80645 | 0.80153 | 0.80060 | 0.80051 | 0.80040 | 0.80033 | 0.80006 |
| $y = 0.9$ | 0.90367 | 0.90089 | 0.90034 | 0.90029 | 0.90023 | 0.90019 | 0.90003 |
| $y = 1.0$ | 1.0 | 1.0 | 1.0 | 1.0 | 1.0 | 1.0 | 1.0 |

The influence of the $\alpha$ memory factor (the fractional order of the derivative in relation to time) on the heat transfer is presented in Figure 3. The curves in Figure 3 highlight the difference between the fluid temperature corresponding to the Fourier law of thermal flux ($\alpha = 0$) and that corresponding to the generalized law of the thermal flux ($0 < \alpha < 1$).

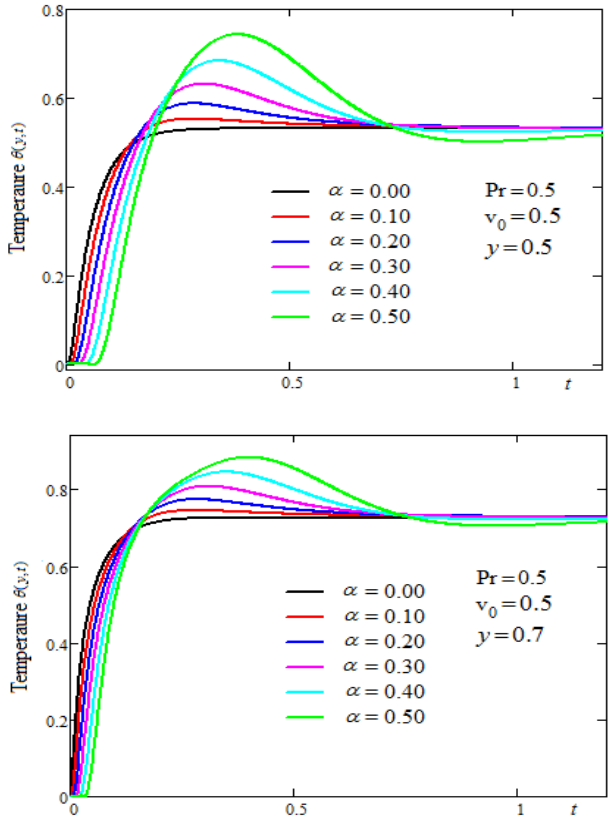


**Figure 3.** The influence of $\alpha$ on $\theta(y,t)$.

For small values of the time t, the temperature values decrease when the fractional memory parameter increases. This is due to the time variation in the memory kernel having large values for t tending to zero and, thus, the damping of temperature gradients is stronger. For time values close to zero, the temperature will have maximum values in the case of thermal transport, based on Fourier's law. After a certain critical moment, the maximum temperature values are obtained for the model based on the generalized heat flow law. Obviously, with increasing time values, the fluid temperature tends towards the post-transition value. The evolution of the temperature field is significantly influenced by the values of the fractional parameter $\alpha$. The modification of the values of the fractional parameter leads to the modification of the weight function values from the generalized definition of the thermal flow, thus to the modification of the thermal diffusion process.

Note that, as expected, the temperature has higher values in the vicinity of the heated wall $y = 1$.

Figures 4 and 5 show the combined effects of injection/suction and thermal memory on the heat transfer. In the case of injection ($v_0 > 0$), the fluid temperature is increasing with the thermal memory parameter $\alpha$, while for suction ($v_0 < 0$) and large values of the thermal memory parameter, the fluid temperature is decreasing in area closed to the wall $y = 0$, and it is increasing in the other one area. As seen in Equation (30), the $v_0$ parameter characterizes the advection phenomenon; therefore, changing the sign of the parameter $v_0$ leads to changing the direction of the advection current from the warm wall to the inside or vice versa; therefore, to significant variations in time of the fluid temperature.

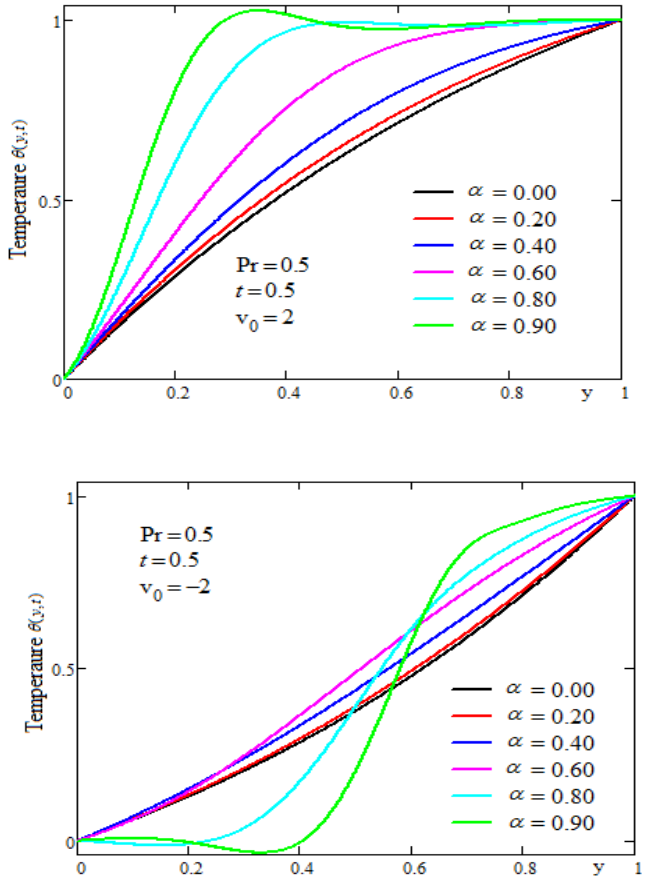


**Figure 4.** Combined effects of the thermal memory and injection/suction on the fluid temperature.

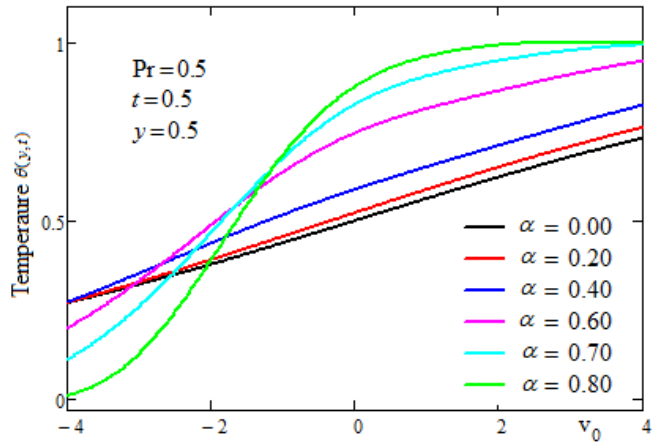


**Figure 5.** Effects of the thermal memory and injection/suction on the fluid temperature.

The influence of the thermal memory parameter $\alpha$ on the fluid velocity and magnetic field is highlighted by the curves shown in Figures 6–9. The numerical values used in drawing the graphs in these figures were obtained for $f(t) = 1, \mathrm{Pr} = 0.5,\ p_m = 0.8,\ q_m = 0.3,\ M_0 = 1.4, \lambda_0 = 0.2, \beta_1 = \beta_2 = \beta_3 = \beta 4 = 0.2$. The curves in Figures 6 and 7 show that the movement of the fluid is attenuated by the increase in the values of the fractional parameter $\alpha$. The justification for this property is due to that the temperature values decrease with the increase in the fractional parameter $\alpha$ and, as a consequence, the values of the buoyancy force are decreasing. The main movement of the fluid is in the direction of the axis of the channel with the primary velocity $u(y,t)$, which reaches its maximum in the central area of the channel in a position close to the heated wall. The profiles of the secondary velocity $w(y,t)$ highlight the fact that the secondary movement of the fluid is much slower than the main one.

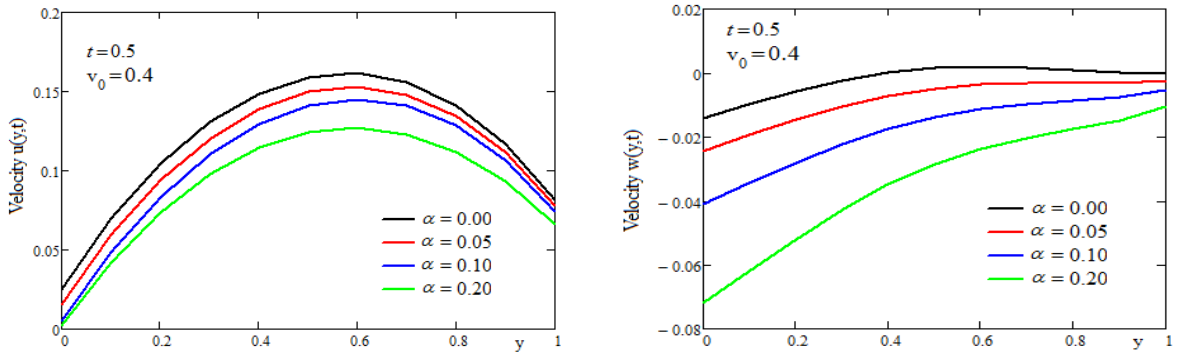


**Figure 6.** Profiles $u(y,t)$ and $w(y,t)$ for different values of the thermal memory parameter $\alpha$.

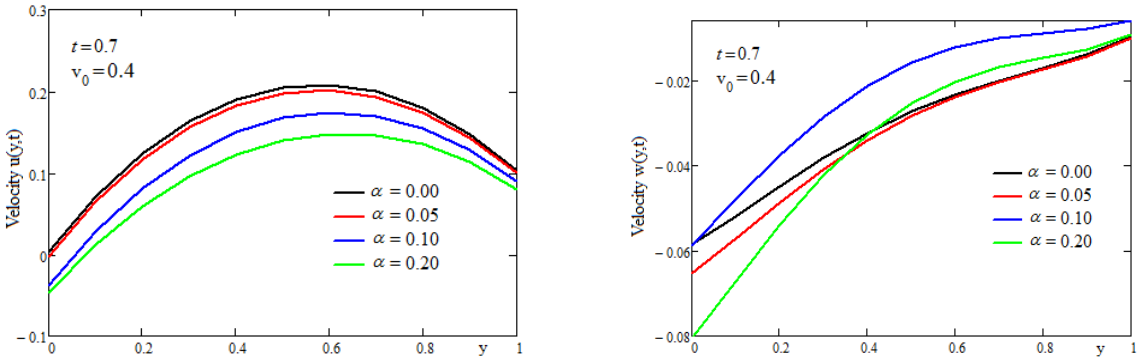


**Figure 7.** Profiles $u(y,t)$ and $w(y,t)$ for different values of $\alpha$.

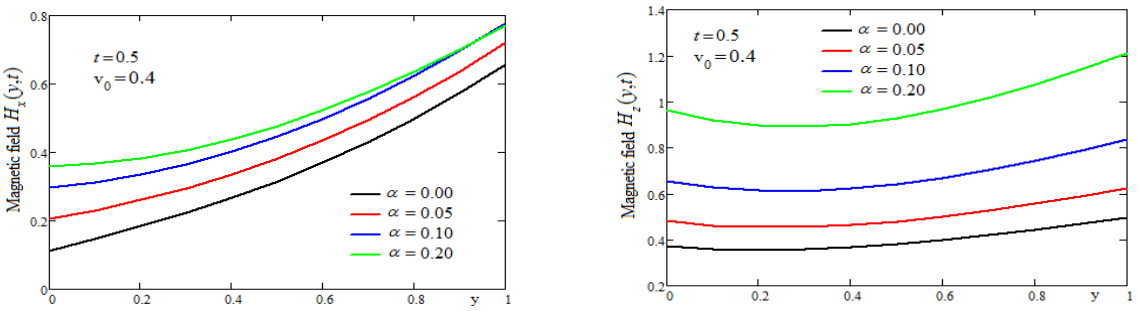


**Figure 8.** Profiles of the induced magnetic field $H_x(y,t)$ $H_z(y,t)$, and for different values of $\alpha$.

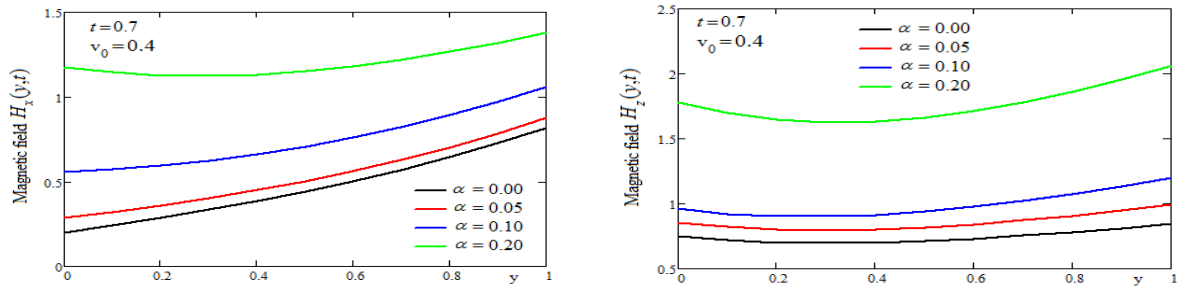


**Figure 9.** Profiles of the induced magnetic field $H_x(y,t)$ $H_z(y,t)$, and for different values of $\alpha$.

Figures 8 and 9 show the influence of the thermal memory parameter on the components of the induced magnetic field. It can be seen that the magnetic field strength increases with the fractional parameter $\alpha$. This will have the effect of slowing down the movement of the fluid at high values of the fractional parameter.

## 5. Conclusions

Effects of the thermal memory on the transient magneto-hydrodynamic buoyancy-driven flow of linear viscous fluids in a rectangular channel with permeable and conducting walls taking into account the effects of magnetic induction, ion slip and Hall current have been semi-analytically investigated.

The hydro-magnetic flow analysis has been carried out for the asymmetry heating of walls combining with suction/injection. The temperature of one of the walls of the channel is time-dependent, while on the other wall, the temperature is constant. Therefore, the studied model could offer solutions for a large class of theoretical/practical problems.

The Laplace transform has been used by researchers to successfully arrive at analytical solutions for temperature, velocity and induced magnetic field in the Laplace domain. They discovered numerical solutions in the real domain by inverting the Laplace transforms using the Stehfest method. The generalized thermal process technique is based on a novel fractional constitutive equation that accounts for both the fluid's hydro-magnetic behavior and the historical influence of the temperature gradient on the thermal process.

The influence of thermal memory on heat transfer, fluid movement and magnetic induction was highlighted by comparing the solutions of the fractional model with the classic one based on Fourier's law.

As expected, the thermal memory parameter $\alpha$ has a significant influence on the heat transfer and the hydro-magnetic behavior of the fluid. This parameter could give solutions for the optimal modeling of some practical heat transfer problems.

**Author Contributions:** Conceptualization, N.A.S.; Methodology, D.V.; Software, B.A.; Formal analysis, D.V.; Resources, A.A.E.-D.; Supervision, A.A.E.-D.; Project administration, B.A. All authors have read and agreed to the published version of the manuscript.

**Funding:** This research work was supported by King Saud University through Researchers Supporting Project number: RSPD2023R650, King Saud University Riyadh, Saudi Arabia.

**Data Availability Statement:** Not applicable.

**Acknowledgments:** The authors extend their appreciation to King Saud University for funding this research through Researchers Supporting Project number: RSPD2023R650, King Saud University Riyadh, Saudi Arabia.

**Conflicts of Interest:** The authors declare no conflict of interest.

**Nomenclature**

| | |
|---|---|
| $c_p$ | Specific heat at constant pressure |
| $d$ | Distance between walls |
| $\vec{g}$ | Acceleration due to gravity |
| $\vec{H} = (H_x, H_0, H_z)$ | Dimensionless magnetic field |
| $\vec{V} = (u, -v_0, w)$ | Dimensionless velocity field |
| $k$ | Thermal conductivity |
| Pr | Prandtl number |
| $q$ | Dimensionless thermal flux |
| $\theta$ | Dimensionless temperature |
| $\beta$ | Coefficient of thermal expansion |
| $\mu$ | Coefficient of viscosity |
| $\rho$ | Fluid mass density |
| $\nu = \mu/\rho$ | Kinematic viscosity |
| $\mu_e$ | Magnetic permeability |
| $\sigma$ | Electrical conductivity |
| $\beta_e$ | Hall parameter |
| $\beta_i$ | Ion slip current |

**Appendix A**

1. Parameters $a_{ij}(s)$ in Equation (64) are

$$a_{11}(s) = r_m\gamma_0^4(s) - (1+r_m)\gamma_0^3(s) + \left[(1+r_m)s + M_0^2 - \mathrm{v}_0^2\right](\gamma_0^2(s) + w^2(s)) + [r_m w(s) + 4r_m\gamma_0^2(s) - (1+r_m)\gamma_0(s)]w^2(s) + s^2 + 2\mathrm{v}_0\gamma_0(s);$$

$$a_{12}(s) = (1+r_m)w^3(s) + 3(1+r_m)\gamma_0^2(s)w(s) - 2(1+r_m)\gamma_0(s)w^2(s) - 2r_m\gamma_0(s)w(s)\left(2w^2(s) + 2\gamma_0^2(s) - \gamma_0(s)w(s)\right) - 2\left[(1+r_m)s + M_0^2 - \mathrm{v}_0^2\right]r_0(s)w(s) - 2\mathrm{v}_0(s)w(s);$$

$$a_{21}(s) = (1+r_m)w^3(s) + 3(1+r_m)\gamma_0^2(s)w(s) - 4r_m\gamma_0^3(s)w(s) - 2r_m\gamma_0(s)w^3(s) + 2\left[(1+r_m)s + M_0^2 - \mathrm{v}_0^2\right]\gamma_0(s)w(s) - 2\mathrm{v}_0(s)w(s);$$

$$a_{22}(s) = r_m w^4(s) + 3r_m\gamma_0^2(s)w^2(s) - 2r_m\gamma_0(s)w^3(s) + r_m\gamma_0^4(s) + 3r_m\gamma_0^2(s)w^2(s) - (1+r_m)\gamma_0^3(s) - 3(1+r_m)\gamma_o(s)w^2(s) - \left[(1+r_m)s + M_0^2 - \mathrm{v}_0^2\right](w^2(s) + \gamma_0^2(s)) + s^2 + 2\mathrm{v}_0 s w(s).$$

2. The roots of Equation (65) are given by [21]

$$X_{1,2}(s) = -\frac{(1+r_m)\mathrm{v}_0}{4r_m} - T(s) \pm \frac{1}{2}\sqrt{\frac{q(s)}{T(s)} - 2p(s) - 4T^2(s)},$$

$$X_{3,4}(s) = -\frac{(1+r_m)\mathrm{v}_0}{4r_m} + T(s) \pm \frac{1}{2}\sqrt{-\frac{q(s)}{T(s)} - 2p(s) - 4T^2(s)},$$

where

$$p(s) = -\frac{(1+r_m)s + M_0^2 - \mathrm{v}_0^2}{r_m} - \frac{3}{8}\left(\frac{(1+r_m)\mathrm{v}_0}{r_m}\right)^2,$$

$$q(s) = \left(\frac{(1+r_m)\mathrm{v}_0}{2r_m}\right)^3 + \left(\frac{(1+r_m)\mathrm{v}_0}{2r_m}\right)\frac{(1+r_m)s + M_0^2 - \mathrm{v}_0^2}{r_m} - \frac{2\mathrm{v}_0 s}{r_m},$$

$$\Delta_0(s) = \left[(1+r_m)s + M_0^2 - \mathrm{v}_0^2\right]^2 + 6(1+r_m)\mathrm{v}_0^2 s + 12r_m s^2,$$

$$\Delta_1(s) = -2[(1+r_m)s + M_0^2 - \mathrm{v}_0^2]^3 - 18(1+r_m)\mathrm{v}_0^2[(1+r_m)s + M_0^2 - \mathrm{v}_0^2]s + 27(1+r_m)^2\mathrm{v}_0^2 s^2 + 54r_m\mathrm{v}_0^2 s^2 + 72r_m[(1+r_m)s + M_0^2 - \mathrm{v}_0^2]s^2,$$

$$Q(s) = \left[\frac{1}{2}\left(\Delta_1(s) + \sqrt{\Delta_1^2(s) - 4\Delta_0^3(s)}\right)\right]^{\frac{1}{3}},$$

$$T(s) = \frac{1}{2}\left(\sqrt{-\frac{2}{3}p(s) + \frac{1}{3r_m}\left(Q(s) + \frac{\Delta_0(s)}{Q(s)}\right)}\right).$$

3. The matrices in Equation (70) are

$$\boldsymbol{M} = (m_{ij})i, j = 1,2,3,4$$

$$m_{1j} = \lambda_0 X_j(s) - 1,\ \mathrm{j} = 1,2,3,4,$$

$$m_{2j} = [\lambda_0 X_j(s) + 1]\exp(X_j(s)),\ \mathrm{j} = 1,2,3,4,$$

$$m_{3j} = \frac{1}{M_0 X_j(s)}[\beta_1 X_j(s) + \beta_2][s - \mathrm{v}_0 X_j(s) - X_j^2(s)],\ j = 1,2,3,4,$$

$$m_{4j} = \frac{\exp(X_j(s))}{M_0 X_j(s)}[\beta_3 X_j(s) + \beta_4][s - \mathrm{v}_0 X_j(s) - X_j^2(s)],\ j = 1,2,3,4,$$

$$\boldsymbol{C} = [C_1(s)C_2(s)C_3(s)C_4(s)]^T,$$

$$\boldsymbol{D} = [D_{11}(s)\ \mathrm{D}_{21}(s)\ \mathrm{D}_{31}(s)\ \mathrm{D}_{41}(s)]^T,$$

$$D_{11}(s) = \exp(\gamma_0(s))[\lambda_0\gamma_0(s)\overline{\mathrm{v}}_{p_1}(s) - \lambda_0 w(s)\overline{\mathrm{v}}_{p_2}(s) - \overline{\mathrm{v}}_{p_1}(s)],$$

$$D_{21}(s) = \left\{\lambda_0[\gamma_0(s)\overline{\mathrm{v}}_{p_1}(s) - w(s)\overline{\mathrm{v}}_{p_2}(s)] - \overline{\mathrm{v}}_{p_1}(s)\right\}\cosh(w(s)) + \left\{\lambda_0[\gamma_0(s)\overline{\mathrm{v}}_{p_2}(s) - w(s)\overline{\mathrm{v}}_{p_1}(s)] - \overline{\mathrm{v}}_{p_2}(s)\right\}\sinh(w(s)),$$

$$D_{31}(s) = \exp(\gamma_0(s))\left\{[\beta_1\gamma_0(s) - \beta_2]\overline{H}_2(s) - \beta_1 w(s)\overline{H}_1(s)\right\},$$

$$D_{41}(s) = [\beta_3\gamma_0(s)\overline{H}_1(s) - \beta_3 w(s)\overline{H}_2(s) - \beta_4\overline{H}_1(s)]\sinh(w(s)) + [\beta_3\gamma_0(s)\overline{H}_2(s) - \beta_3 w(s)\overline{H}_1(s) - \beta_4\overline{H}_2(s)]\cosh(w(s)).$$

## References


1. Davidson, P.A.; Belova, E.V. *An Introduction to Magnetohydrodynamics*, 2nd ed.; Cambridge University Press: Cambridge, UK, 2016.
2. Ghosh, S.K.; Nandi, D.K. Magnetohydrodynamic Fully Developed Combined Convection Flow between Vertical Plates Heated Asymmetrically. *J. Tech. Phys.* **2000**, *41*, 173–185.
3. Jha, B.K.; Apere, C.A. Magnetohydrodynamic Free Convective Couette Flow with Suction and Injection. *J. Heat Transf.* **2011**, *133*, 092501. [CrossRef]
4. Hamza, M.M.; Usman, I.G.; Sule, A. Unsteady/Steady Hydromagnetic Convective Flow between Two Vertical Walls in the Presence of Variable Thermal Conductivity. *J. Fluids* **2015**, *2015*, 358053. [CrossRef]
5. Shao, Z.; Shah, N.A.; Tlili, I.; Afzal, U.; Khan, M.S. Hydromagnetic free convection flow of viscous fluid between vertical parallel plates with damped thermal and mass fluxes. *Alex. Eng. J.* **2019**, *58*, 989–1000. [CrossRef]
6. Singh, K.D.; Pathak, R. Effect of rotation and Hall current on mixed convection MHD flow through a porous medium filled in a vertical channel in presence of thermal radiation. *Ind. J. Pure Appl. Phys.* **2012**, *50*, 77–85.
7. Singh, J.K.; Vishwanath, S. Hall and induced magnetic field effects on MHD buoyancy-driven flow of Walters' B fluid over a magnetised convectively heated inclined surface. *Int. J. Ambient. Energy* **2021**, *43*, 4444–4453. [CrossRef]
8. Imran, M.A.; Shah, N.A.; Khan, I.; Aleem, M. Applications of non-integer Caputo time fractional derivatives to natural con-vection flow subject to arbitrary velocity and Newtonian heating. *Neural Comp. Appl.* **2018**, *30*, 1589–1599. [CrossRef]
9. Ahmed, N.; Shah, N.A.; Vieru, D. Natural convection with damped thermal flux in a vertical circular cylinder. *Chin. J. Phys.* **2018**, *56*, 630–644. [CrossRef]

10. Jha, B.K.; Aina, B.; Ajiya, A. MHD natural convection flow in a vertical parallel plate microchannel. *Ain Shams Eng. J.* **2015**, *6*, 289–295. [CrossRef]
11. Jha, B.K.; Aina, B.; Ajiya, A.T. Role of suction/injection on MHD natural convection flow in a vertical microchannel. *Int. J. Energy Technol.* **2015**, *7*, 30–39.
12. Pantokratoras, A. Fully developed laminar free convection with variable thermophysical properties between two open-ended vertical parallel platesheated asymmetrically with large temperature differences. *J. Heat Transfer* **2006**, *128*, 405–408. [CrossRef]
13. Narahari, M. Oscillatory plate temperature effects of free convection flow of dissipative fluid between long vertical parallel plates. *Int. J. Appl. Math. Mech.* **2009**, *5*, 30–46.
14. Hristov, J. A transient flow of a non-Newtonian fluid modelled by a mixed time-space derivative: An improved integral-balance approach. In *Mathematical Methods in Engineering—Theory*; Tas, K., Baleanu, D., Machado, J.A.T., Eds.; Springer International Publishing: Cham, Switzerland, 2018.
15. Hristov, J. Diffusion models of heat and momentum with weakly singular kernels in the fading memories: How the integral-balance method can be applied? *Therm. Sci.* **2015**, *19*, 947–957. [CrossRef]
16. Baleanu, D.; Diethelm, K.; Scalas, E. *Fractional Calculus Models and Numerical Methods*; World Scientific: Singapore, 2012.
17. Tarasov, V.E. *Fractional Dynamics: Applications of Fractional Calculus to Dynamics of Particles, Fields and Media, Nonlinear Physical Science*; Springer and Higher Education Press: Berlin/Heidelberg, Germany; Beijing, China, 2011.
18. Atanackovic, T.M.; Pilipovic, S.; Stankovic, B.; Zorica, D. *Fractional Calculus with Applications in Mechanics: Vibrations and Diffusion Processes*; Challamel, N., Ed.; ISTE Ltd.: London, UK; John Wiley & Sons, Inc.: New York, NY, USA, 2014.
19. Vieru, D.; Fetecau, C.; Ahmed, N.; Shah, N.A. A generalized kinetic model of the advection-dispersion process in a sorbing medium. *Math. Model. Nat. Phenom.* **2021**, *16*, 39. [CrossRef]
20. Kuznetsov, A. On the Convergence of the Gaver—Stehfest Algorithm. *SIAM J. Numer. Anal.* **2013**, *51*, 2984–2998. [CrossRef]
21. Faucete, W.M. A geometric interpretation of the solution of the general quartic polynomial. *Amer. Math. Montly* **1996**, *103*, 51–57. [CrossRef]